NMR IN BIOMEDICINE, VOL. **10**, 165–170 (1997)

Simultaneous Assessment of Flow and BOLD Signals in Resting-State Functional Connectivity Maps

Bharat B. Biswal,* Joel Van Kylen and James S. Hyde

Biophysics Research Institute, Medical College of Wisconsin, 8701 Watertown Plank Road, PO Box 26509, Milwaukee, WI 53226, USA

We have recently demonstrated using functional magnetic resonance imaging the presence of synchronous low-frequency fluctuations of signal intensities from the resting human brain that have a high degree of temporal correlation ($p < 0.0001$) both within and across the sensorimotor cortex. A statistically significant overlap between the resting-state functional connectivity map and the task-activation map due to bilateral finger tapping was obtained. Similar results have been obtained in the auditory and visual cortex. Because the pulse sequence used for collecting data was sensitive to blood flow and blood oxygenation, these low-frequency fluctuations of signal intensity may have arisen from variations of both. The objective of this study was simultaneously to determine the contribution of the blood oxygenation level signal and the flow signal to physiological fluctuations in the resting brain using the flow-sensitive alternating inversion recovery pulse sequence. In all subjects, the functional connectivity maps obtained from BOLD had a greater coincidence with task-activation maps than the corresponding functional connectivity maps obtained from blood-flow signals at the same level of statistical significance. Results of this study suggest that while variations in blood flow might contribute to functional connectivity maps, BOLD signals play a dominant role in the mechanism that gives rise to functional connectivity in the resting human brain. © 1997 John Wiley & Sons, Ltd.

NMR in Biomed. **10**, 165–170 (1997) No. of Figures: 3 No. of Tables: 1 No. of References: 22

Keywords: functional connectivity; resting brain; blood flow; blood oxygenation

Received 28 January 1997; accepted 4 February 1997

INTRODUCTION

It has been observed by various groups that signal intensities in a time course of functional magnetic resonance imaging (fMRI) images in a resting human brain vary by about 1–2% over the mean.[1–4] Frequency bands corresponding to the fundamental cardiac and respiration rates along with higher harmonics have been observed. In addition, low frequencies (< 0.1 Hz) have been observed.[5] After filtering the high-frequency components including the respiration and the cardiac rates, a statistically significiant temporal correlation within the sensorimotor cortex, both ipsilaterally and contralaterally, was obtained during the resting-state. Only a few pixel time courses outside the sensorimotor cortex exhibited significant temporal correlation with sensorimotor pixel time courses. A substantial overlap between resting-state functional connectivity maps and task-activation maps during bilateral finger tapping was observed.[5] Similar results have been obtained in the visual and the auditory cortex.[6–8] These results have been replicated and extended by a second research group.[9]

Low-frequency fluctuations in the cortex originating from blood flow and oxygenation have been observed in animal models using a variety of techniques, including laser Doppler flowmetry (LDF),[10–12] fluoro-reflectometry[13, 14] and polarographic measurement of brain tissue PO_2 with micro electrodes.[15–17] Previous reports have suggested that synchronous fluctuations may be a general cortical phenomenon representing the functional connection of cortical areas.[18]

Although temporal correlation between functionally related regions of the brain has been demonstrated, the mechanisms underlying the observations are not completely understood. It is currently believed that these low-frequency fluctuations play an important role in maintaining an optimal balance between blood flow and oxygenation consumption. In this study, we used the flow-sensitive alternating inversion recovery (FAIR) pulse sequence[19, 20] for simultaneous assessment of the contributions of blood flow and blood oxygenation to resting-state functional connectivity maps.

EXPERIMENTAL

Imaging using FAIR

Experiments were performed using a 3 T/60 Bruker scanner and a home built three-axis balanced-torque head gradient coil with an endcapped birdcage RF transmit–receive coil. In all experiments, the RF power deposition and field switching rate were kept below levels specified by the US Food and Drug Administration. All functional MRI (fMRI)

* Correspondence to: B. B. Biswal.
Contract grant sponsor: NIH; *contract grant number:* MH51358; *contract grant number:* CA41464.
Contract grant sponsor: Whitaker Foundation

 CCC 0952–3480/97/040165–06 $17.50

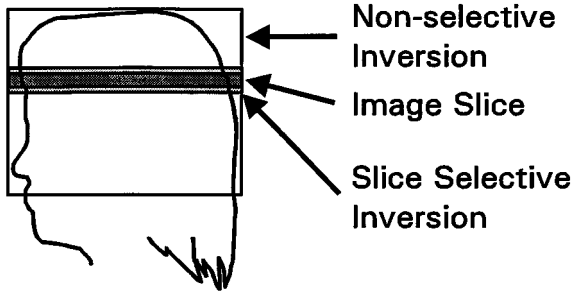

Figure 1. FAIR is a pulsed arterial spin-labeling technique that alternates between slice-selective and nonslice-selective inversion. All images are obtained using the same imaging slice. The nonslice selective images are BOLD weighted. The slice selective images are BOLD plus flow weighted.

data including both task-activation and resting-state experiments were collected using the FAIR pulse sequence.[19,20] Because this method has been described in detail elsewhere, it is only briefly reviewed here.

FAIR is a pulsed arterial spin labelling technique that uses endogenous water as a tracer by alternating between slice-selective and non slice-selective inversion, as shown in Fig. 1. After the inversion, a time delay before the image is collected allows blood to move into the imaging slice. The blood that moves in during slice selective inversion is fresh and enhances the signal, while blood that moves in during nonslice-selective inversion is inverted blood and does not change the signal. The even numbered nonslice-selective images are blood oxygenation level (BOLD) weighted. All odd numbered images in the image sequence are slice-selective BOLD plus flow weighted. Subtracting every odd numbered image from the succeeding even-numbered image results in a time series of images that is flow weighted.

Human subjects

Four subjects (three males and one female) between 14 and 29 years of age with no known neurological disorders, head trauma, contraindication to MR, or medication were scanned. The subjects were informed about the nature of the experiment and asked to sign consent forms. They were self-identified as right-handed. The subjects were told that they would be required to perform bilateral finger tapping at a self-paced rate, but were not given specific information about timing. Plastic earphones with air-conducting tubing were used to deliver instructions.

Data acquisition

Sessions started with the acquisition of high resolution anatomic images in axial and saggital planes with the fast spin-echo (FSE) pulse sequence, with $TR = 500$ ms, $TE = 10$ ms, $FOV = 24$ cm, and matrix size $= 256 \times 256$. On the basis of these images, an axial plane-of section passing through the motor cortex was defined for each volunteer, and resting-state as well as task-activation time courses of 240 FAIR images were acquired using a $TR = 2000$ ms, $TE = 40$ ms, and slice-selective inversion width $= 14$ mm. Other imaging parameters were $FOV = 24$ cm, matrix size $= 64 \times 64$, and slice thickness $= 7$ mm. The TI value was 1400 ms, which suppresses the signal at 3 T from the CSF and blood.

The first FAIR scan was in the nonstimulus (resting) condition while the subjects were naive to the succeeding tasks. They were instructed to close their eyes and refrain from any cognitive, sensory, or motor activity. During the second scan, subjects were instructed to perform bilateral finger tapping for a 60 s period followed by a 60 s period of rest for four cycles. During bilateral finger tapping, each finger was touched with the thumb sequentially in a self-paced manner.

Data analysis

Each resting-state time-course data set was broken into two data sub-sets: the first contained even numbered images that were nonslice-selective BOLD weighted, and the second was formed by subtracting every odd numbered image from the succeeding image, resulting in flow-weighted images. Although the TR of the FAIR sequence was 2000 ms, the effective sampling rate was 0.25 Hz since every other image was processed for BOLD and flow. This results in a frequency bandwidth of 0.125 Hz. A low-pass filter with a cut-off frequency at 0.1 Hz was used to reduce the respiratory frequency and other high frequency components of the signal. Some portion of the cardiac component must in principle be aliased and should appear in the low-frequency range. Since the cardiac frequencies are expected to be present throughout the cortex, all pairwise correlations of pixel time-courses would be affected similarly and the patterns of correlations would be unaffected. In our studies of physiological fluctuations the effects of aliasing have been a concern, but thus far have not been detected.

Task-activation data sets were processed in a similar fashion, resulting in BOLD-weighted and flow-weighted subsets. An ideal box-car waveform corresponding to the stimulus presentation was cross-correlated with every pixel time-course on a pixel-by-pixel basis for both subsets. A activation correlation-coefficient (*acc*) threshold of 0.5 after the Bonferroni correction corresponds to a statistical significance of $p < 0.001$. It was used to detect both task-induced BOLD signal changes and flow signal changes. All pixels that passed this threshold were considered activated and belonging to the motor cortex.

The BOLD task-activation map was used to analyze the BOLD resting-state data subset, and the flow task-activation and resting-state data were analyzed similarly. Consider for example the BOLD data. For each subject, the number of pixels in the left motor cortex that passed the *acc* threshold, n_L, was determined; and similarly for the right motor cortex n_R. The number of pixels in other brain tissue (n_O) was also determined. The maps of the activated pixels were superimposed onto the anatomic images to determine the location of the sensorimotor cortices. The corresponding pixels from the resting-state BOLD time-series were selected and cross-correlated with every other time-course in the BOLD resting-state image series on a pixel-by-pixel basis.

Activated and corresponding resting-state time-course data sets were selected for standard parametric statistics. Time and frequency analysis were performed on the data sets. The mean and standard deviation of each of the data sets were calculated. The Fourier transforms of all time courses were also calculated.

The method of analysis of pixel time courses from resting

brain used in this paper is based on an earlier paper of ours.[7] This method calculates an optimum coincidence between the task-activation map and resting-state functional connectivity map along with the resting correlation coefficient (*rcc*). The pairwise correlation coefficient (*PCC)* matrix is formed by cross-correlating every pixel time course (say *n*) with every other pixel (*n*) in the brain, resulting in a matrix dimensionality of $n \times n$. Let

$$n = n_R + n_L + n_O \tag{1}$$

where n = mean number of pixels in the brain, n_R = mean number of pixels in the right motor cortex, n_L = mean number of pixels in the left motor cortex, and n_O = mean number of pixels in the brain outisde the motor cortex. Submatrices of dimensionality $n_R \times n_R$ and $n_L \times n_L$ were used to investigate ipsilateral correlation. Submatrices $n_R \times n_L$ and $n_L \times n_R$ are redundant; they contain contralateral correlation information. Submatrices $n_R \times n_O$ and $n_L \times n_O$ were studied to detect possible correlations involving the sensorimotor system with other regions that were not identified during task acquisition. All diagonal entries on the PCC matrix are unity (i.e. correlation of a pixel time course with itself) and were excluded from the statistics. The PCC matrix is symmetric and only the lower diagonal terms (non-redundant) were used for statistical analyses.

By choosing an appropriate resting correlation coefficient (*rcc*), an image can be formed by cross-correlating the time course of any pixel within the sensorimotor cortex with all other time courses. The degree of correspondence of this image with the image formed by task activation is dependent on the choice of the *rcc* threshold. This idea of adjusting the *rcc* for best fit between a pair of images can be extended to the PCC matrix. There are $n_R + n_L$ rows, using a pixel time-course within the sensorimotor cortex as one member of the correlation pair, corresponding to $n_R + n_L$ possible images. The *rcc* threshold that yields the best possible fit of these images, taken together as a group, to the task-activation map is determined by adjusting it to maximize the spatial coincidence coefficient, *SCC*, which we define in eq. (2):

$$SCC = \frac{1}{3}\left(\frac{n_{LL}}{n_L{}^2 + n_{LO}} + \frac{n_{RR}}{n_R{}^2 + n_{RO}} + \frac{2n_{LR}}{2n_L n_R}\right) \tag{2}$$

Here n_{LL} is the number of off-diagonal entries in the $n_L \times n_L$ submatrix above the *rcc* threshold, and similarly for n_{RR}, n_{LO} and n_{RO}. Well-delineated maxima in *SCC* were observed in data from all subjects with a representative *rcc* threshold value of 0.3, corresponding to a statistical significance $p < 0.05$. The definition in eq. (2) assures that the value of *SCC* lies between zero and one.

This method leads to an unambiguous determination of the *rcc* threshold. Measures of ipsilateral task-rest coincidence are then given by eqs (3) and (4):

$$SCC_{LL} + \frac{n_{LL}}{(n_L{}^2 + n_{LO})} \tag{3}$$

$$SCC_{RR} + \frac{n_{RR}}{(n_R{}^2 + n_{RO})} \tag{4}$$

and for contralateral connectivity by

$$SCC_{LR} = SCC_{RL} = \frac{2n_{LR}}{(2n_L n_R + n_{LO} + n_{RO})} \tag{5}$$

$$SCC_{RLO} = \left(\frac{n_{LO}}{n_O n_L}\right) + \left(\frac{n_{RO}}{n_O n_R}\right) \tag{6}$$

The *SCC* values in eqs (3)–(5) lie between zero and one and can be expressed as percentages. Terms SCC_{LL}, SCC_{RR} and $SCC_{LR,RL}$ are nearly the same as the terms $\bar{n}_{LL}/\bar{n}_L$, $\bar{n}_{RR}/\bar{n}_R$ and n_{LR}/n_L introduced by Biswal *et al.*[5] They differ only by the exclusion of diagonal self-correlation unity values from the statistics. Terms n_{LO} and n_{RO} penalize the statistics when resting correlation coefficients from pixels in the 'other' brain tissue pass the *rcc* threshold. The purpose of this analytical approach is to arrive at an objective procedure for setting the *rcc* threshold for the best correspondence of brain regions activated by the task with brain regions defined by spatial correlation of physiological fluctuations. Equation (6) is a measure of the extent of correlated pixel time courses in other tissue. It is mathematically identical to the term $(\bar{n}_{LO} + \bar{n}_{RO})/n_O$ used by Biswal *et al.*[5] but the notation is changed to accommodate the introduction of the *PCC* matrix.

This entire process was repeated using flow-weighted task-activated and resting-state data.

RESULTS

Figure 2(a) shows a representative low-pass filtered time course from a pixel identified as lying within the primary motor cortex of a subject during bilateral finger tapping. An activation correlation-coefficient (*acc*) threshold of 0.5 was used for identifying activated pixels. BOLD- and FLOW-weighted signal variations during task activation are shown horizontally adjacent. Typical signal intensities varied by about 5 and 6%. Representative numbers of activated pixels within and outside the sensorimotor cortex are $n_R = 25$, $n_L = 25$ and $n_O = 1000$. Similar numbers were also found in the flow weighted task-activation map.

During resting acquisitions, the signal intensity varied by about 1–2% of baseline. It was seen that the flow-weighted signal variations during rest had a greater standard deviation than the corresponding BOLD-weighted signal variations. Representative resting-state pixel time-course from the motor cortex obtained with BOLD-weighting and flow-weighting are shown in Fig. 2(b). Fourier analysis performed on these two time-course plots indicated a dominant low-frequency fluctuation centered at around 0.06 Hz in both. The magnitude of the low-frequency fluctuation obtained with BOLD weighting was of higher magnitude than with flow weighting (Fig. 2(c).

Table 1 shows the spatial coincidence coefficient (*SCC*) data from the sensorimotor cortex for BOLD- and flow-weighing data from all four subjects. The *rcc* threshold values varied from 0.31 to 0.44 for BOLD and 0.28 to 0.37 for flow over the four subjects. For every subject, the *rcc* value was greater for BOLD data than for flow. The percentage of activated pixels in the left hemisphere that had significantly correlated synchronous fluctuations during rest ranged from 63 to 84% for the BOLD-weighted images

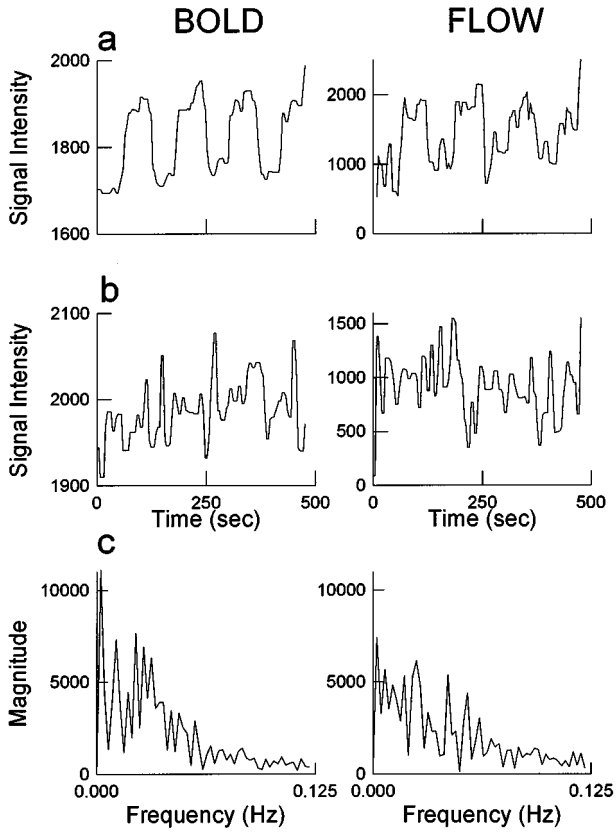

Figure 2. Pixel time-course signal intensity changes from a representative pixel in the motor cortex: (1) task activation; (b) resting state. Fourier transform magnitudes of resting-state time courses are shown in (c).

and 33 to 53% for flow-weighted images. Similarly in the right cortex, *SCC* ranged between 66 and 81% and 29 and 51% in the BOLD-weighted and flow-weighted images, respectively. The ipsilateral spatial coincidence coefficients (SCC_{LL} and SCC_{RR}) were about the same with BOLD-weighted data showing much higher coincidence of resting-state maps with task-activation maps than was obtained with flow-weighted data Across hemispheres SCC_{LR} the percentages ranged from 43 to 54% and 17 to 41% for BOLD- and flow-weighted data, respectively.

The higher values of *rcc* and for SCC_{LL}, SCC_{RR}, and SCC_{LR} for BOLD relative to flow coupled with lower values for SCC_{LRO} (which arises from stray pixels) leads to the conclusion that BOLD weighting is preferred for functional connectivity maps.

Figure 3(a) and (b) show task-activated images from subject no. 4 during bilateral finger tapping using BOLD and flow weighting. The corresponding resting-state functional connectivity maps are shown in Fig. 3(c) and (d). Close correspondence between Fig. 3(a) and (c) was observed. However, the *SCC* was much less between (b) and (d). It can be seen in Fig. 3(d) that the resting-state flow-weighted functional connectivity map is greatly altered and that many pixel time courses from regions outside the sensorimotor cortex pass the *rcc*.

DISCUSSION

In our earlier studies demonstrating resting-state functional connectivity maps in the sensorimotor cortex, a $T_2^\star$-weighted EPI pulse sequence with *TR* of 250 ms was used, resulting in time-course data sets that were 16 times larger than in the present study. As a result, the signal-to-noise ratio (SNR) was greater. The detected signal variations were, however, sensitive to both blood flow and oxygenation, and the relative contributions from each of the two components was not determined. The present study demonstrates the presence of BOLD- and flow-weighted synchronous low-frequency signal intensity variations in the sensorimotor cortex of the human brain during rest. Synchronous low-frequency fluctuations were observed both within and across associated regions of the sensorimotor cortex. It was demonstrated, comparing BOLD- and flow-weighted maps, that BOLD weighting results in substantially superior resting-state functional connectivity maps. While flow-weighted signals are correlated, the connectivity maps show less coincidence with task-activation maps and exhibit more stray pixels.

In an earlier study we demonstrated that respiratory hypercapnia reversibly suspends synchronous low-frequency fluctuations.[21] The low-frequency fluctuations observed in MR in the sensorimotor cortex (and other functionally related regions of the human brain) are similar in nature to fluctuations observed using LDF in the rat cortex; these fluctuations were thought to be secondary to fluctuations in neuronal activity. In the present study we have demonstrated that the BOLD-weighted variations in signal intensity play a dominant role in the formation of resting-state functional connectivity maps, showing that these maps are not formed due to vasomotion as has been recently suggested by Mitra *et al.*[22] This lends further support to our hypothesis that the fluctuations are neuronal in nature.

The spatial width of the slice-selective inversion recovery slab used in this study was about two times greater than the

Table 1. Correlation coefficient data from resting brain

Subject	Weighting	Threshold (*rcc*)	SCC_{LL} (%)	SCC_{RR} (%)	SCC_{LR} (%)	SCC_{LRO} (%)
1	BOLD	0.44	67	68	52	2.7
	Flow	0.37	42	47	23	3.4
2	BOLD	0.31	63	66	43	3.1
	Flow	0.28	33	29	17	4.3
3	BOLD	0.41	71	69	49	1.9
	Flow	0.37	39	38	28	2.8
4	BOLD	0.33	84	81	54	2.3
	Flow	0.31	53	51	41	3.5
Average	BOLD	0.37 ± 0.06	71.2 ± 9.1	71.0 ± 6.7	52.0 ± 8.8	2.5 ± 0.4
	Flow	0.33 ± 0.05	41.7 ± 8.4	41.3 ± 9.8	27.3 ± 10.2	3.5 ± 0.4

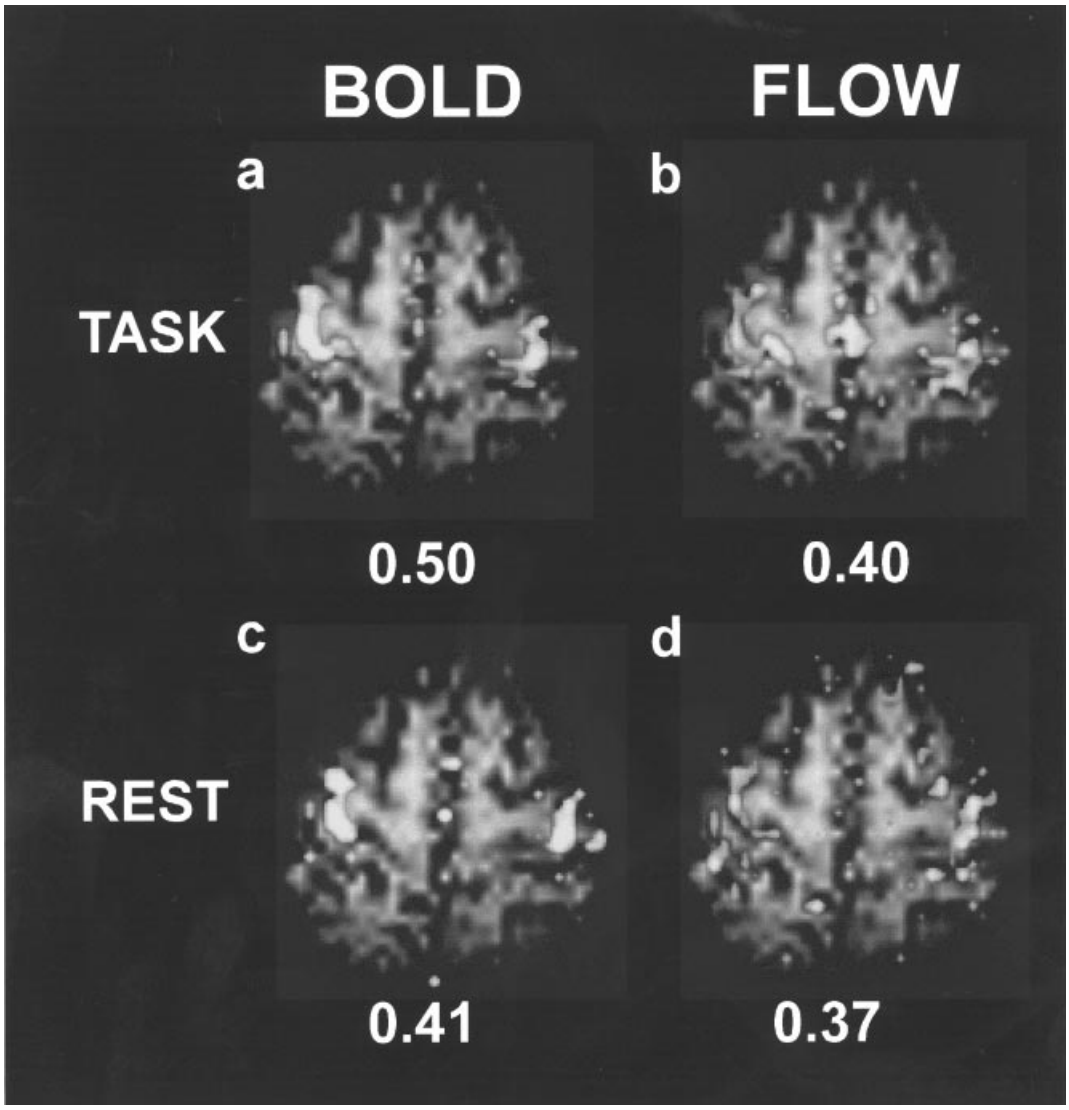

Figure 3. Comparison of maps obtained using the FAIR pulse sequence during task-activation and resting-state FMRI. Thresholds are indicated. Close correspondence between BOLD-weighted task-activation map (a) and BOLD-weighted resting-state functional connectivity map (c) was observed. However, the coincidence between the flow-weighted task-activation map (b) and resting-state functional connectivity map (d) was much less. See text for details.

width of the imaging slice (14 vs 7 mm) and was not as well defined since there were no RF lobes. It is possible that the use of very well-matched inversion and imaging slices would result in improved flow-weighted functional connectivity maps. One can also imagine a modified FAIR sequence in which the selective and nonselective pulses were replaced by two slice-selective inversion pulses of different spatial width. Such a sequence could be expected to give information on flow effects involving vessels of differing size and orientation.

BOLD-weighted functional connectivity maps obtained here were superior relative to flow-weighted maps, but the acquisition time was relatively long because of the use of a *TR* value of 2000 ms. BOLD weighting arises from two effects in the present study—the long *TR* and the use of a nonselective inversion recovery pulse. Inversion recovery pulse sequences can be written with shorter *TR* values, and this is a possible direction for future studies.

The *TI* values of CSF and of blood are similar and signals from both fluids were suppressed by the *TI* value used here. Although suppression of flow-weighting effects has been demonstrated to be clearly desirable, it is possible that the improved functional connectivity maps obtained in the present work arise in part from the suppression of BOLD signals from CSF that are associated with draining veins.

The functional significance of these observations remains to be competely explained. Synchronous low-frequency fluctuations have been observed in animal models using a number of different techniques. It has been suggested by Bressler[18] that temporal signals in synchrony might play an important role in determining cortical output involving functionally related regions.

It is very unlikely that the resting-state functional connectivity maps arise from imagined finger tapping, not only because subjects were naive to the task, but also because we have demonstrated in other studies that functional connectivity between functionally related regions is a general phenomenon. In addition, previous studies on imagined motor tasks have reported activation in the SMA but not in the primary motor areas, in contrast to our results.

This study is preliminary in nature. A small number of volunteers has been studied. Not all controls have been performed. A systematic error or artifact of respiratory,

cardiac or other cyclic physiological phenomena is excluded since the synchronous fluctuations are not distributed over the entire slice. Because of the low signal-to-noise ratio in the resting acquisition, use of high field scanners such as 3 T as well as use of relatively large voxels are advantageous.

Acknowledgements

We would like to thank Peter A. Bandettini for useful discussions about FAIR. This work was supported by grants MH51358 and CA41464 from the National Institutes of Health and by an award from the Whitaker Foundation.

REFERENCES

1. Weisskoff, R. M., Baker, J., Belliveau, J., Davis, T. L., Kwong, K. K., Cohen, M. S. and Rosen, B. R. Power spectrum analysis of functionally-weighted MR data: what's in the noise? *Proceedings, SMRM, 12th Annual Meeting,* New York, p. 7 (1992).
2. Jezzard, P., LeBihan, D., Cuenod, D., Pannier, L., Prinster, A. and Turner, R. An investigation of the contribution of physiological noise in human functional MRI studies at 1.5 tesla and 4 tesla. *Proceedings, SMRM, 12th Annual Meeting,* New York, p. 1 392 (1992).
3. Biswal, B. B., De Yoe, E. A., Jesmanowicz, A. and Hyde, J. S. Time-frequency analysis of functional EPI time-courses. *Proceedings, SMRM, 12th Annual Meeting,* New York, p. 1392 (1992).
4. Biswal, B. B., DeYoe, E. A. and Hyde, J. S. Reduction of physiological fluctuations in FMRI using digital filters. *Magn. Reson. Med.* **35**, 107–113 (1996).
5. Biswal, B. B., Yetkin, F. Z., Haughton, V. M. and Hyde, J. S. Functional connectivity in the motor cortex of resting human brain using echo-planar MRI. *Magn. Reson. Med.* **34**, 537–541 (1995).
6. Biswal, B. B., DeYoe, E. A., Yetkin, F. Z., Haughton, V. M. and Hyde, J. S. Temporal correlation of FMRI signal may reveal brain connectivity. *Society of Neuroscience.* Abstr., p. 905 (1995).
7. Biswal, B. B., DeYoe, E. A., Yetkin, F. Z., Haughton, V. M. and Hyde, J. S. Functional connectivity of the human auditory cortex studied with FMRI (submitted).
8. Biswal, B. B., Yetkin, F. Z., Haughton, V. M. and Hyde, J. S. Functional connectivity in the auditory cortex studied with FMRI. *Neuroimage* **3**, S305 (1996).
9. Lowe, M. J., Mock, B. J. and Sorenson, J. A. Resting state fMRI signal correlation in multi-slice EPI. *Neuroimage* **3**, S257 (1996).
10. Hudetz, A. G., Roman, R. J. and Harder, D. R. Spontaneous flow oscillations in the cerebral cortex during acute changes in mean arterial pressure. *J. Cereb. Blood Flow Metab.* **12**, 491–499 (1992).
11. Golanov, E. V., Yamamoto, S. and Reis, D. J. Spontaneous waves of cerebral blood flow associated with patterns of electrocortical activity. *Am. J. Physiol.* **266**, R204–214 (1994).
12. Hudetz, A. G., Smith, J. J., Lee, J. G., Bosnjak, Z. J. and Kampine, J. P. Modification of cerebral laser-Doppler flow oscillations by halothane, PCO_2, and nitric oxide synthase blockade. *Am. J. Physiol.* **269**, H114–H120 (1995).
13. Dora, E. and Kovach, A. G. B. Metabolic and vascular volume oscillations in the cat cerebral cortex. *Acta Physiol. Acad. Sci. Hung.* **57**, 261–275 (1980).
14. Vern, B. A., Schuette, W. H., Leheta, B., Juel, V. C. and Radulovacki, M. Low-frequency oscillations of cortical oxidative metabolism in waking and sleep. *J. Cereb. Blood Flow Metab.* **8**, 215–226 (1988).
15. Moskalenko, Y. E. *Biophysical Aspects of Cerebral Circulation.* Pergamon, Oxford (1980).
16. Halsey, J. H. Jr and McFarland, S. Oxygen cycles and metabolic autoregulation. *Stroke* **5**, 219–225 (1974).
17. Cooper, R., Crow, H. J., Walter, W. G. and Winter, W. L. Regional control of cerebral vascular reactivity and oxygen supply in man. *Brain Res.* **3**, 174–191 (1966).
18. Bressler, S. Large-scale cortical networks and cognition. *Brain Res. Rev.* **20**, 288–304 (1996).
19. Kwong, K. K., Chesler, D. A., Weisskoff, R. M., Donahue, K. M., Davis, T. L., Ostergaard, L., Campbell, T. A. and Rosen, B. R. MR perfusion studies with T_1-weighted echo planar imaging. *Magn. Reson. Med.* **34**, 878–887 (1995).
20. Kim, S. G. Quantification of relative cerebral blood flow change by flow-sensitive alternating inversion recovery (FAIR) technique: application to functional mapping. *Magn. Reson. Med.* **34**, 293–301 (1995).
21. Biswal, B. B., Hudetz, A. G., Yetkin, F. Z., Haughton, V. M. and Hyde, J. S. Hypercapnia reversibly suppresses low-frequency fluctuations in the human motor cortex during rest using echo-planar MRI. *J. Cereb. Blood Flow Metab.* **17**, 301–308 (1997).
22. Mitra, P. P., Ogawa, S., Hu, X. and Ugurbil, K. The nature of spatiotemporal changes in functional MRI. *Proceedings, ISMRM, 4th Annual Meeting,* New York, p. 1869 (1996).

